

Dependence of Intramolecular Electron-Transfer Rates on Driving Force, pH, and Temperature in Ammineruthenium-Modified Ferrocycytochromes *c*

James F. Wishart,^{*,†} Ji Sun,^{†,‡} Myung Cho,[‡] Chang Su,^{†,||} and Stephan S. Isied^{*,‡}

Department of Chemistry, Brookhaven National Laboratory, Upton, New York 11973-5000, and the Department of Chemistry, Rutgers, the State University of New Jersey, Piscataway, New Jersey 08855

Received: August 13, 1996; In Final Form: November 18, 1996[®]

Several ruthenium ammine complexes were used to modify horse-heart cytochrome *c* at histidine-33, creating a series of (NH₃)₄(L)Ru–Cyt *c* derivatives (L = H₂O/OH[−], ammonia, 4-ethylpyridine, 3,5-lutidine, pyridine, isonicotinamide, *N*-methylpyrazinium) with a wide range of driving forces for Fe-to-Ru electron transfer (−Δ*G*[°] = −0.125 to +0.46 eV). Electron-transfer rates and activation parameters were measured by pulse radiolysis using azide or carbonate radicals. The driving-force dependence of electron-transfer rates between redox centers of the same charge types obeys Marcus–Hush theory. The activationless rate limit for all of the ruthenium derivatives except the *N*-methylpyrazinium complex is 3.9 × 10⁵ s^{−1}. Thermodynamic parameters obtained from nonisothermal differential pulse voltammetry show that the electron-transfer reactions are entropy-driven. The thermodynamic and kinetic effects of phosphate ion binding to the ruthenium center are examined. The rate of intramolecular electron transfer in (NH₃)₄(isn)Ru^{III}–Cyt *c*^{II} decreases at high pH, with a midpoint at pH 9.1.

Introduction

Electron-transfer proteins covalently substituted with ruthenium complexes bound to specific residues on the surface of the protein have been very useful in providing a detailed understanding of the intramolecular electron-transfer process across protein matrixes.^{1–9} The kinetic stability of the ruthenium centers allows one to carry out detailed studies of the intramolecular electron-transfer process as a function of a variety of changes in the protein medium. Studies of the reversibility of the kinetics of intramolecular electron transfer and the effect of pressure on the kinetics and thermodynamics of a number of these molecules have been carried out.^{6,7} Agreement between values derived from the thermodynamics and kinetics experiments increased confidence in the results.²

In this paper the effect of driving force, pH, and buffer media on the thermodynamics and kinetics of intramolecular electron transfer for a series of complexes, *trans*-[L(NH₃)₄Ru–Cyt *c*] (L = H₂O/OH[−], ammonia, 4-ethylpyridine, 3,5-lutidine, pyridine, isonicotinamide, *N*-methylpyrazinium), will be presented. Small but reproducible effects of pH and buffer medium on the rates have been examined. The dependence of the rate of intramolecular electron transfer on driving force for the series of related ruthenium tetraammine complexes obeys the Marcus–Hush theory, with deviations for highly charged ruthenium complexes and ligand radical-based Ru(II) reducing agents.

Experimental Section

Potassium trisoxalatocobaltate (K₃[Co(ox)₃]·3.5H₂O), was prepared by the method of Bailar.¹⁰ Ruthenium-modified cytochromes *trans*-(NH₃)₄Ru(L)–Cyt *c*, L = NH₃,¹¹ pyridine,¹ and isonicotinamide,¹ were prepared as previously reported.

Modified cytochromes with L = 3,5-lutidine or 4-ethylpyridine were prepared identically to the pyridine derivative. Gel filtration chromatography in the preparations described below was performed using Sephadex G-25 gel filtration columns (1 × 50 cm) equilibrated with 50 mM potassium phosphate buffer (pH 7.0), and elutions were done with the same buffer while monitoring at 254 nm. Amicon YM05 membranes were used for ultrafiltration.

Modification of Horse Heart Cytochrome *c* with *cis*-(NH₃)₄Ru(OH₂)₂]²⁺. Purified Hh Cyt *c* (~100 mg, 0.008 mmol) in ~5 mL of 50 mM potassium phosphate buffer, pH 7.0, was reduced with excess ascorbic acid (~2 mg). To remove the excess ascorbic acid, the reduced protein was run through a Sephadex G-25 gel filtration column (see above). The reduced protein was collected, equilibrated with 10 mM Tris/HCl buffer (pH 6.5), and concentrated to ~2 mL by ultrafiltration. The presence of residual ascorbic acid was detected by adding 0.1 M AgNO₃ to the eluent. The absence of a black colloidal silver suspension confirmed that the reducing agent was removed. The concentrated protein was transferred to a dialysis bag (Spectrum Med. Ind., MW 6000–8000 cutoff) containing several pieces of Zn/Hg and a stir bar.

In a bubble flask, 50 mg of *cis*-(NH₃)₄RuCl₂]Cl (0.18 mmol) in 10 mL of degassed 10 mM Tris/HCl buffer (pH 6.5) was reduced by the addition of several pieces of fresh zinc amalgam while bubbling with argon for 1 h. Using a gastight syringe, the reduced ruthenium solution was transferred to a flask containing the dialysis bag with the reduced cytochrome *c*, and the solution was stirred at room temperature. Pieces of zinc amalgam were placed in the flask to ensure that the ruthenium complex remained reduced. After 17 h, the reaction solution was concentrated to ~3 mL by ultrafiltration and purified by gel filtration. The eluted protein solution was washed with 50 mM potassium phosphate buffer (pH 7.0) and concentrated to ~5 mL by ultrafiltration. Yields of the modified protein ranged from 5 to 10%.

Modification of Hh Cytochrome *c* with *cis*-(NH₃)₄Ru-(Mepz)(OH₂)₂]²⁺. Purified Hh Cyt *c* (~100 mg (0.008 mmol) in ~5 mL of 50 mM potassium phosphate buffer (pH 7.0) was reduced with excess ascorbic acid (~2 mg) and separated from

[†] Brookhaven National Laboratory.

[‡] Rutgers, the State University of New Jersey.

^{*} To whom correspondence should be addressed. E-mail: wishart1@bnl.gov.

[†] Present address: IGEN, Inc., 16020 Industrial Dr., Gaithersburg, MD 20877.

^{||} Present address: Department of Molecular Sciences, Hoffmann-La Roche Co., 340 Kingsland Ave., Nutley, NJ 07110-1199.

[®] Abstract published in *Advance ACS Abstracts*, January 1, 1997.

the excess ascorbic acid by gel filtration. The reduced protein was equilibrated with 100 mM HEPES buffer (pH 7.0) and concentrated to ~2 mL by ultrafiltration. The absence of residual ascorbic acid was confirmed by adding 0.1 M AgNO₃ to the eluent as described above. The concentrated protein (in 100 mM HEPES buffer) was transferred to a bubble flask, and argon was bubbled gently for 30 min. Approximately 0.1 mmol of solid *cis*-[(NH₃)₄Ru^{II}(Mepz)Cl]Cl₂ was added to the reduced cytochrome *c* solution, and the reaction was allowed to proceed with stirring in the dark under argon for 72 h at room temperature. The product was then separated from starting materials by gel filtration. The collected protein solution was washed with 50 mM potassium phosphate buffer, (pH 7.0) and concentrated to ~5 mL by ultrafiltration. Yields of the modified protein varied from 3 to 8%.

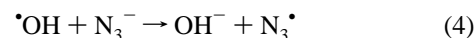
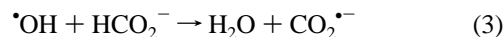
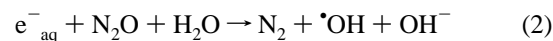
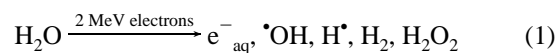
Electrochemistry. Differential pulse voltammetry was carried out using a BAS 100B electrochemical analyzer (Bioanalytical Systems, West Lafayette, IN). A three-electrode configuration was used, consisting of a gold disk working electrode (MF 2014, Bioanalytical Systems), a platinum wire auxiliary electrode, and a saturated sodium chloride calomel reference electrode (236 mV vs NHE). The gold disk working electrode was polished with a 0.05 μm alumina slurry (Union Carbide, Indianapolis, IN). In all the electrochemical measurements for both the native and modified proteins, 4,4'-dipyridyl disulfide was used to modify the gold electrode surface, and the cyt *c* concentrations were ~0.1–0.3 mM in 50 mM potassium phosphate (pH 7.0) solution. To accurately measure the peak separations of closely spaced DPV waves for the ruthenated cytochromes, the digitized voltammograms were fitted on a Macintosh IIfx computer using Igor 1.28 (WaveMetrics, Inc., Lake Oswego, OR) as described previously.⁶

Differential pulse voltammograms were recorded as a function of temperature between 5 and 45 °C using a water-jacketed electrochemical cell from Bioanalytical Systems, Inc. (West Lafayette, IN). The cell was placed inside a polystyrene foam pint-bottle shipping jacket packed with glass wool. The temperature of the cell was continuously monitored with a Teflon-sleeved, type-J thermocouple probe. For these experiments, the reference electrode (SSCE, saturated sodium chloride calomel) was connected to the cell by a 3-in. salt bridge which protruded outside the insulation. No particular effort was made to maintain the reference electrode at 25 °C, however, since we are concerned only with the temperature dependence of the potential difference between the ruthenium and cytochrome couples and not their individual variations with respect to the reference couple.

Cyclic voltammetry measurements listed in Table 3 were performed on a BAS 100-A electrochemical analyzer with a glassy carbon electrode and a standard saturated calomel reference electrode.

Pulse Radiolysis. Electron pulse-radiolysis transient-absorption experiments were carried out with the 2 MeV Van de Graaff accelerator at Brookhaven National Laboratory using a PC-controlled, CAMAC-based data acquisition and control system. The experiments were done using an all-quartz pulse radiolysis cell consisting of a 50 mL reservoir with an outlet which drains into a 20 mm long, 10 mm high, 5 mm deep rectangular optical cell where the sample is irradiated (through the short dimension) and probed by light passing through the long dimension (2.0 and 6.1 cm path lengths). Irradiated solutions are drained from the cell after use, so the solution in the reservoir remains fresh until it is used. Carbon dioxide radical anion, CO₂^{•-}, was produced by the reaction of radiolytically generated hydroxyl radical (•OH) with formate ion (0.1 M HCOONa) in N₂O-

saturated water (reactions 1–3). Azide radical, N₃[•], was



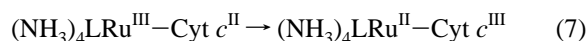
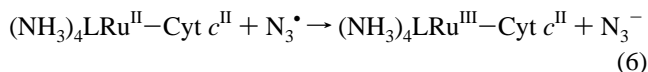
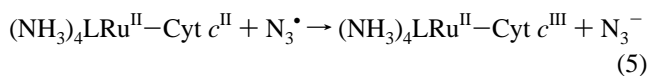
produced by the reaction of •OH with azide ion (1 mM NaN₃) in N₂O-saturated water (reactions 1, 2, and 4). Similarly, carbonate radical (CO₃^{•-}) was formed from the reaction of •OH with bicarbonate and/or carbonate anions. Radiolytic dose levels were chosen such that the concentrations of oxidizing or reducing radicals produced in a single shot were no more than 15% of the cytochrome concentration. Radiolysis pulse widths were between 60 and 120 ns. The buffer was 50 mM sodium phosphate (pH 7.0) except where noted.

Preparations of fully reduced ruthenium-modified cytochromes *c* for pulse radiolysis experiments were carried out in an argon-filled glovebox (Vacuum Atmospheres). The modified cytochrome *c* was reduced with an excess of sodium dithionite (50 mM), which was then removed by repeated ultrafiltration over a 3000 dalton molecular-weight-cutoff membrane using argon-saturated 50 mM phosphate buffer. Meanwhile, 15–50 mL of phosphate buffer solution containing 1 mM sodium azide was saturated with N₂O in a pulse radiolysis reservoir cell. The reduced cytochrome *c* solution was diluted to the desired concentration and placed in a syringe for transfer out of the glovebox. The solution was introduced to the pulse radiolysis cell through a rubber septum via an 18-gauge platinum needle. The final concentration of ruthenated cytochrome *c* in the pulse radiolysis solution (normally 2–20 μM) was determined by using a Hewlett-Packard 8452A diode array spectrophotometer to measure the absorbance of samples drained from the radiolysis cell (after the first two samples were discarded) as fully reduced protein after addition of sodium ascorbate (ε₄₁₆ = 129 100 M⁻¹, ε₅₅₀ = 27 000 cm⁻¹ M⁻¹).¹²

In the case of L = H₂O/OH⁻, reductive pulse radiolysis with CO₂^{•-} such as originally performed¹³ on the L = NH₃ complex was used to measure the reaction rate at pH 7.0.

Results and Discussion

Measurement of Electron-Transfer Rates. Intramolecular electron-transfer rates were measured by an oxidative scheme using pulse-radiolytically generated azide radical (E° = +1.33 V vs NHE¹⁴) or carbonate radical (E° = +1.5 V vs NHE¹⁵). Direct oxidation of the ferrocyclochrome center by N₃[•] (eq 5, *k* ≈ 1 × 10⁹ M⁻¹ s⁻¹) is slower than oxidation at the ruthenium center (eq 6, *k* ≈ 2 × 10⁹ M⁻¹ s⁻¹), resulting in a good yield of the kinetic intermediate which decays by intramolecular electron transfer (eq 7).¹⁶



Previous work¹ has shown that cytochrome-bound ruthenium-(III) ammine complexes with substituted pyridines disproportion-

TABLE 1: Observed Rate Constants, Activation Parameters, and Thermodynamic Values for Intramolecular Electron Transfer in Tetraammine(L)ruthenium-Modified Horse-Heart Cytochrome *c*^a

L (t/c)	ET direction	ΔG° (eV)	rate (s^{-1} , 25 °C)	ΔH^\ddagger (kcal/mol)	ΔS^\ddagger (eu)	ΔH^{ob} (kcal/mol)	ΔS^{ob} (eu)
NH ₃	Ru→Fe	-0.125	53 ± 2	3.5 ± 0.1	-39.0 ± 0.4 ^c		
	Fe→Ru	+0.125	0.40 ± 0.01	12.5 ± 0.2	-18.3 ± 0.7 ^d	9.0 ± 0.1	20.7 ± 0.4
4-ethylpyridine							
trans-	Fe→Ru	-0.08	76 ± 1	9.0 ± 0.1	-19.8 ± 0.3		
3,5-lutidine							
trans-	Fe→Ru	-0.09	85 ± 1	9.2 ± 0.1	-18.9 ± 0.3	2.6 ± 0.1	15.2 ± 0.4
pyridine							
trans-	Fe→Ru	-0.11	126 ± 5	8.8 ± 0.1	-19.3 ± 0.3 ^e	3.6 ± 0.1	20.7 ± 0.4
isonicotinamide ^f							
trans-	Fe→Ru	-0.18	440 ± 26	7.3 ± 0.1	-22.0 ± 0.4 ^e	2.13 ± 0.06	21.2 ± 0.2
cis-	Fe→Ru	-0.18	440	6.2 ± 0.3	-26 ± 1 ^e		
H ₂ O							
cis-	Ru→Fe	-0.27	720 ± 40				
N-methylpyrazinium							
cis-	Fe→Ru	-0.46	1300				

^a Conditions: 50 mM pH 7.0 sodium phosphate buffer except where noted. ^b Thermodynamic data (for the Fe→Ru direction) determined by nonisothermal DPV. In the case of L = NH₃ the values obtained from the activation parameters are identical, except the error limits are 0.2 kcal mol⁻¹ and 0.8 cal deg⁻¹ mol⁻¹. ^c Reference 13. The standard deviations were recalculated from the data in Table 1 therein. ^d Reference 2. ^e Reference 1. ^f Thermodynamic values measured for the *trans* complex.

tionate at neutral and weakly acidic pH. The problem can be avoided by keeping the ruthenium complex reduced until the electron transfer intermediate is formed.

Reaction 7 was followed by measuring the bleaching of the Cyt *c*^{II} absorption at 550 nm and the increase in absorbance of the (NH₃)₄LRu^{II}-His33 complex at 504 or 432 nm, which are isosbestic points for the Cyt *c*^{II} and Cyt *c*^{III} spectra. Typical kinetic traces have been published previously.¹ The intramolecular electron-transfer rates for all of the ruthenium derivatives are tabulated in Table 1. All of the observed rates were found to be invariant with concentration over the range 1–20 μM.

Intramolecular heme reduction in (NH₃)₅Ru-Cyt *c* can also be observed by oxidative pulse radiolysis. In the case of L = NH₃, the reduction potential of the ruthenium center is lower than that of the heme center, so reaction 7 is driven from right to left. A 4 μM solution of (NH₃)₅Ru^{III}-Cyt *c*^{II} in N₂O-saturated 0.1 M phosphate buffer and 0.1 M sodium bicarbonate (pH 7.5) was reduced with 4.8 μM Ru(NH₃)₆²⁺. The oxidation of the heme center by carbonate radical and subsequent intramolecular rereduction by the pendant ruthenium center were followed at 550 nm. A series of kinetic traces showing the effect of repeated pulses on the same sample is included in the supporting material. The kinetic intermediate (NH₃)₅Ru^{II}-Cyt *c*^{III} is formed as a minor fraction; direct carbonate radical oxidation of the ruthenium center to give the thermodynamically favored product (NH₃)₅Ru^{III}-Cyt *c*^{II} proceeds more rapidly. Repeated pulsing depletes the Ru^{II}, allowing oxidation of the heme center to compete and reveal the intramolecular rereduction process. The observed rate for nine observations similar to the middle three traces in the supporting figure is 49 ± 3 s⁻¹, in good agreement with the value of 53 s⁻¹ obtained by the reductive method.¹³ When the solution was diluted to 2 μM (NH₃)₅Ru^{II}-Cyt *c*^{II} with additional phosphate/bicarbonate solution, the observed rate was 48 ± 3 s⁻¹.

Dependence of Intramolecular ET Rates on Driving Force.

In one formalism,¹⁷ the rate of intramolecular electron transfer k_{et} may be expressed as the product of k_{el} , the electronic transmission coefficient, ν_n , the effective nuclear frequency along the reaction coordinate, and an activation term involving the free energy barrier of reorganization, ΔG_r^* :

$$k_{et} = k_{el}\nu_n \exp(-\Delta G_r^*/RT) \quad (8)$$

$$\Delta G_r^* = (\lambda_{12}/4)(1 + \Delta G^\circ/\lambda_{12})^2 \quad (9)$$

TABLE 2: Calculation of the Free Energy Barriers to Reorganization for Intramolecular Electron Transfer in Tetraammine(L)ruthenium-Modified Horse-Heart Cytochrome *c*

modified cyt + direction of ET	ΔG° (eV)	λ_M (eV)	λ_{Ru} (eV)	λ_{12} (eV)	ΔG_r^* (eV)	k_{obs} (s ⁻¹)
(NH ₃) ₅ Ru→Fe	-0.125	1.0	1.2	1.1	0.216	53
(NH ₃) ₅ Ru←Fe	0.125	1.0	1.2	1.1	0.341	0.40
(NH ₃) ₄ (etpy)Ru←Fe	-0.08	1.0	1.0	1.0	0.212	76
(NH ₃) ₄ (lut)Ru←Fe	-0.09	1.0	1.0	1.0	0.207	85
(NH ₃) ₄ (py)Ru←Fe	-0.11	1.0	1.0	1.0	0.198	126
(NH ₃) ₄ (isn)Ru←Fe	-0.18	1.0	1.0	1.0	0.168	440
(NH ₃) ₄ (H ₂ O)Ru→Fe	-0.27	1.0	1.2	1.1	0.157	720
(NH ₃) ₅ Ru→Fe <i>Ck</i> ^a	-0.18	1.0	1.2	1.1	0.192	154
(NH ₃) ₄ (isn)Ru←Fe <i>Ck</i> ^a	-0.13	1.0	1.0	1.0	0.189	220
(NH ₃) ₄ (Mepz)Ru←Fe ^b	-0.46	1.0	1.0	1.0	0.073	1200
(NH ₃) ₄ (Mepz ⁻)Ru→Fe ^c	-0.28	1.0	1.0	1.0	0.130	630

^a *Candida kreusei*, His-39 attachment. Reference 1. ^b Additional (+) charge on Ru complex. ^c Electron transfer from the ligand-centered Mepz⁻ radical.

To a first approximation, the preexponential terms k_{el} and ν_n in eq 8 are not sensitive to variations in the ligand L in (NH₃)₄-LRu^{II}-Cyt *c*. On the other hand, substitution of different ligands L changes the driving force (ΔG°_{12}) and thereby affects the free energy barrier to reorganization, ΔG_r^* , according to eq 9 (where the reorganization energy $\lambda_{12} = (\lambda_{cyt} + \lambda_{Ru})/2$). Using the measured driving forces and reliable estimates of the reorganization energy contributions from the ruthenium and cytochrome centers, eq 9 can be used to calculate ΔG_r^* for each ruthenium derivative, so that the correlation implied by eq 8 may be tested.

The calculations are summarized in Table 2. The entries in the top part of the table are grouped together because they all involve the same redox centers and charge types.¹⁸ Literature reorganization energies^{17,19} were used: $\lambda_{cyt} = 1.0$ eV and $\lambda_{Ru} = 1.2$ eV (for L = NH₃ and H₂O) and $\lambda_{Ru} = 1.0$ eV for all other complexes. The linear correlation predicted by eq 8 between the natural log of the observed rates and ΔG_r^* can be seen clearly in Figure 1. The slope of the least-squares fit line of all the points in the top part of Table 2 (represented as circles in Figure 1) is $-(1.04 \pm 0.01)/RT$, very close to the theoretical value of $-1/RT$. The activationless rate limit ($k_{max} = k_{el}\nu_n$) is 3.9×10^5 s⁻¹. Using the formula¹⁷ $k_{el}\nu_n = (H_{ab})^2 (4\pi^3/h^2\lambda_{12})^{1/2}$, the electronic coupling matrix element between the reactant

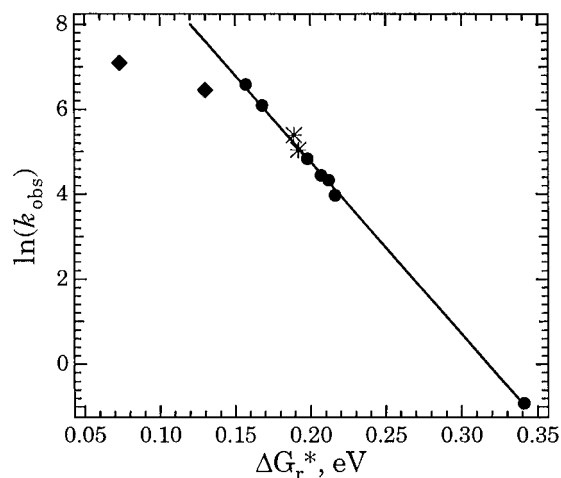


Figure 1. Observed rate constants for intramolecular electron transfer in the tetraammine(L)ruthenium-modified cytochrome *c* systems listed in Table 2, plotted against the calculated free energy barriers to reorganization. The activationless rate limit ($k = k_{el} \nu_n$) obtained through a least-squares linear fit is $3.9 \times 10^5 \text{ s}^{-1}$. The starred points represent *Candida kreusei* derivatives, and the diamonds represent the horse heart *N*-methylpyrazinium complex.

and product states H_{ab} is calculated to be 0.040 cm^{-1} , close to earlier estimates.⁴

The four entries in the lower part of Table 2 are also plotted (as stars or diamonds) in Figure 1 for comparison. The two starred points¹ involve electron transfer from ruthenium complexes bound to His-39 of *Candida kreusei* (*Ck*) cytochrome *c*. Horse heart (Hh) and *Ck* cytochrome *c* are structurally very similar, and the His-33 and His-39 sites are about the same distance from the iron center (11.1 and 12.3 Å, respectively⁴). Analysis of the most-probable electron-transfer “pathways” between the heme and the His-33 and His-39 sites reveals that they both consist of 11 covalent and one hydrogen bond⁴ with nearly identical effective through-bond distances ($n_{\text{eff}} = 13.9$ and 14).⁴ Our results support the conclusion that the coupling in the Hh (His 33) and *Ck* (His 39) cases is similar. The differences in driving force account for the observed rate differences between Hh and *Ck* cytochromes modified with the same ruthenium derivative. Earlier suggestions²⁰ that the effective coupling (H_{ab})² is 3 times higher in the *Ck* case over Hh are not borne out by our observations, particularly in the case of $L = \text{isn}$ where the *Ck* electron-transfer rate is half of that for horse heart.

The diamond symbols in Figure 1 represent electron-transfer rates in the *N*-methylpyrazinium derivative. Intramolecular reduction of the $(\text{NH}_3)_4\text{LRu}^{\text{III}}(\text{N-methylpyrazinium})$ center has a higher reorganization energy²¹ due to an additional positive charge on the ruthenium center, leading to a slower rate than predicted by the correlation (left diamond in Figure 2). In addition, the strongly π -acidic *N*-methylpyrazinium ligand may greatly reduce coupling from Ru to C5 on the imidazole and thence to the heme center and slow the electron-transfer reaction. The final entry in Table 2 is for electron transfer from the ligand-centered radical (formed through the reduction of the $(\text{NH}_3)_4\text{-MepzRu}^{\text{II}}$ center by CO_2^- radical) to the Fe^{III} center. Since the redox site is localized on a ligand of the ruthenium center, the coupling is expected to be less than that for Ru-centered systems, and this expectation is borne out in an observed rate which is lower than the correlation predicts (right diamond).

A plot of $\ln(k_{\text{obs}})$ versus driving force for the same complexes is shown in Figure 2 (Mepz derivative omitted). The figure illustrates the validity of the small correction of the reorganization energy (λ_{12}) for the ruthenium complexes containing

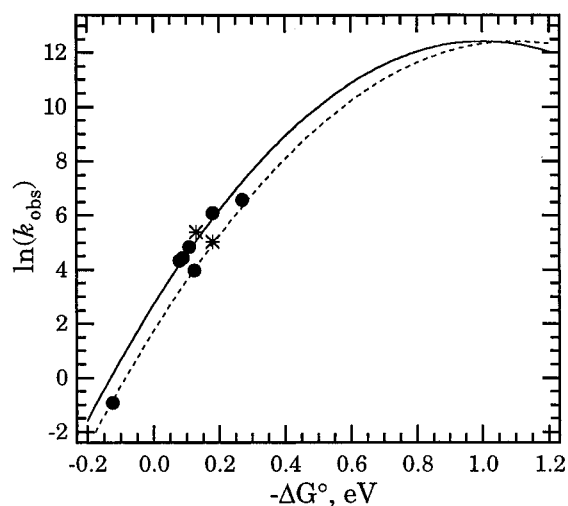
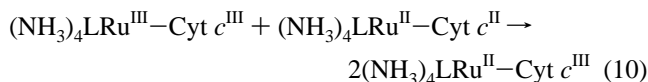


Figure 2. Semilog plot of observed rates as a function of driving force for the compounds listed in top section of Table 2. The two curves correspond to families of systems with slightly different reorganization energies ($L = \text{NH}_3$ and H_2O , $\lambda_{12} = 1.1 \text{ eV}$, dotted line; all others, $\lambda_{12} = 1.0 \text{ eV}$, solid line) and an activationless rate limit of $3.9 \times 10^5 \text{ s}^{-1}$. The starred points represent *Candida kreusei* derivatives.

pyridine derivatives (Table 2).¹⁸ For the theoretical curves in Figure 2, $k_{el} \nu_n = 3.9 \times 10^5 \text{ s}^{-1}$, and λ_{12} is taken to be 1.0 eV for the pyridine derivatives (solid curve), while $\lambda_{12} = 1.1 \text{ eV}$ for $L = \text{NH}_3$ and $\text{H}_2\text{O}/\text{OH}^-$ (dashed curve).

Thermodynamic and Activation Parameters for Intra-protein Electron Transfer. Nonisothermal differential pulse voltammetry was used to determine the difference in peak potentials at 5, 15, 25, 35 and 45 °C for the $\text{Ru}^{\text{III/II}}$ and $\text{Fe}^{\text{III/II}}$ redox couples in $(\text{NH}_3)_4\text{LRu}^{\text{II}}\text{-Cyt } c$, $L = \text{NH}_3$, 3,5-lutidine, pyridine, and isonicotinamide. The data are tabulated and plotted in the Supporting Information, and the resulting reaction enthalpies and entropies are given in Table 1. The results directly apply to the comproportionation reaction:



However, if one assumes that the centers do not interact significantly, the thermodynamic parameters obtained for reaction 10 should also be valid for reaction 7. This is supported by the good agreement of the ΔH° and ΔS° values calculated from the activation parameters² for reaction 7 and its reverse in the case $L = \text{NH}_3$ with the ΔH° and ΔS° values obtained by van't Hoff treatment of the electrochemical data. The data show that Fe-to-Ru electron transfer is entropy-driven (even in the isonicotinamide case). The large increase in entropy is likely to be due in large part to a decrease in electrostriction around the ruthenium center upon reduction. In the case of $L = \text{NH}_3$ the large endothermicity ($\Delta H^\circ = +9.0 \text{ kcal mol}^{-1}$) overrides the entropy increase and drives the reaction in the opposite direction. The reaction enthalpies for ruthenium reduction are significantly smaller in the lutidine, pyridine, and isonicotinamide cases than for ammonia, presumably due to stabilization of Ru^{II} by π -back-bonding.

The fitting procedure used to resolve the overlapping DPV peaks gives clear results when the peaks are distinguishable ($\Delta E_{\text{peak}} \geq 100 \text{ mV}$), however, as the peak separation decreases to the point where one broad peak is observed the possibility of a systematic fitting error affecting the slope of the ΔE_{peak} vs temperature plot must be considered. This difficulty may be present in the case of $L = 3,5\text{-lutidine}$, where ΔS° obtained by the nonisothermal DPV is $\sim 5 \text{ cal K}^{-1} \text{ mol}^{-1}$ less than in the

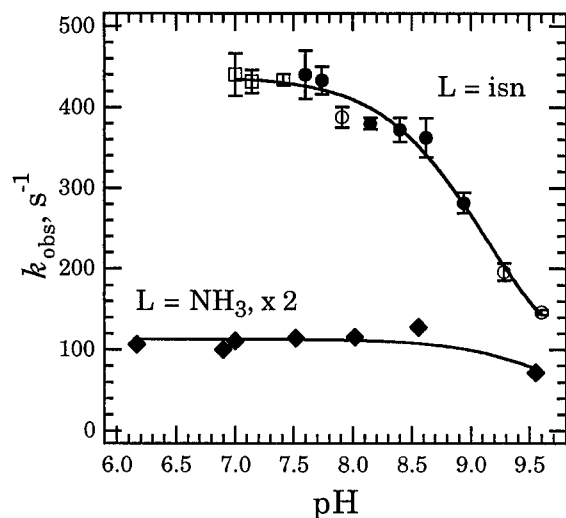


Figure 3. Plot of observed intramolecular electron-transfer rates as a function of pH for *trans*-(NH₃)₄(L)Ru-modified cytochrome *c*, L = NH₃ (Ru-to-Fe) and isn (Fe-to-Ru). Data for L = NH₃ from ref 24. For L = isn, the media are as follows: open squares, 0.1 M phosphate buffer, 1 mM NaN₃; filled circles, 0.1 M phosphate buffer, 0.05 M NaHCO₃; open circles, 0.1 M phosphate buffer, 0.1 M NaHCO₃. In the case of bicarbonate solutions, the pH was varied by bubbling with N₂O to drive off CO₂.

three other cases. We plan to test this result by determining the activation parameters for the uphill Ru-to-Fe electron-transfer reaction using a reductive analogue of the preequilibrium saturation technique employed in ref 2. Comparison of the activation entropies for Fe-to-Ru electron transfer among similar complexes (L = NH₃, py, isn) suggests that the lutidine derivative should not be different from the others in terms of reaction entropy.

The activation enthalpies for Fe-to-Ru electron transfer (Table 1) reflect the decreasing reaction endothermicity (+12.5 to +7.3 kcal mol⁻¹) along the series L = NH₃, 4-ety, 3,5-lut, py, isn. The activation entropies remain essentially constant: -18.3 to -22.0 cal deg⁻¹ mol⁻¹. It is interesting to compare the observed activation parameters with those derived¹⁷ from the Marcus expression for the intramolecular rate constant (eqs 8, 9, 11, and 12) where $\Delta H_r^\ddagger \approx \Delta H_r^*$ and $\Delta S_r^\ddagger \approx \Delta S_r^* + R \ln(k_{el} \nu_n / 10^{13})$:

$$\Delta H_r^* = \lambda/4 + \Delta H^\circ[1 + \Delta G^\circ/\lambda]/2 - (\Delta G^\circ)^2/4\lambda \quad (11)$$

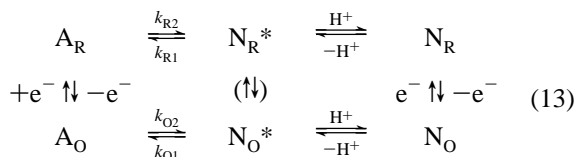
$$\Delta S_r^* = \Delta S^\circ[1 + \Delta G^\circ/\lambda]/2 \quad (12)$$

Applying the above equations to the cases L = NH₃ (downhill), NH₃ (uphill), 3,5-lut, py, isn, one obtains $\Delta H_r^\ddagger_{\text{calc}} = 2.3, 11.3, 6.9, 7.3$, and 6.5 kcal mol⁻¹ and $\Delta S_r^\ddagger_{\text{calc}} = -43.1, -22.4, -26.9, -24.7$, and -25.2 cal K⁻¹ mol⁻¹, respectively. With the exception of 3,5-lutidine where the thermodynamic values are less certain because of overlapping peaks (vide supra), the calculated activation parameters are slightly more negative but in reasonable agreement with those observed.

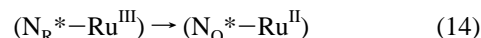
pH Dependence of Intramolecular Electron Transfer. The pH dependence of the intramolecular electron-transfer rate for the L = isonicotinamide case is shown in Figure 3. The azide radical was used to initiate the electron-transfer reaction at lower pH's, while carbonate radical was used at pH 7.6 and above. In all cases, the phosphate buffer concentration was 0.1 M (speciation varies with pH). The rate data show a dramatic transition to much slower rates (limiting rate between zero and 50 s⁻¹) with a midpoint around pH 9.1 ± 0.1. The midpoint does not correspond to the pK_a's of phosphate or bicarbonate

buffers; therefore, the rate decrease is not a consequence of lower driving force induced by anion complexation of the ruthenium moiety. However, the midpoint is similar to the pK_a of the alkaline form of horse heart ferricytochrome *c*.²²

Barker and Mauk²³ have examined the conformational steps involved in the pH-dependent redox equilibria of iso-1 and horse heart cytochrome *c*, which they have described in the following scheme (eq 13), where N and A represent native and alkaline conformations, respectively, and the subscripts R and O represent the reduced and oxidized forms:



As the pH is raised, deprotonation ($N_O \rightleftharpoons N_O^* + H^+$) of some residue(s), possibly lysines, induces conversion of ferricytochrome to the alkaline form in which the Met-80 side chain normally coordinated to the heme is replaced by a nitrogenous ligand ($N_O^* \rightarrow A_O$). In the reduced form of the protein, the Met-bound, deprotonated form N_R^* is favored over the alkaline form, A_R . In the case of the present studies of intramolecular oxidation of the reduced form, the dominant cytochrome species above pH 9.1 would be N_R^* . For some reason, intramolecular oxidation of N_R^* (eq 14, $k \leq 50$ s⁻¹) is much slower than for N_R (eq 7).



The data in Figure 3 imply that the pK_a for N_R may be the same as that of N_O , indicating that the key ionized residue is not sensitive to oxidation state and that the reduction potential for the (N_O^*/N_R^*) couple is essentially the same as the native forms at pH 7. If this is the case, deprotonation of the protein does not affect the driving force for electron transfer as depicted in eq 14.

There are at least two possible explanations for the rate decrease at higher pH. The first reason might be a decrease in driving force at the ruthenium couple, due either to deprotonation of a ligand coordinated to Ru^{III} (ammonia or the imidazole group of His-33) or due to hydrogen bonding from a deprotonated residue (possibly the nearby Lys-22). In either case, the driving force would have to be reduced by 0.12 eV or more to account for the observed rate decrease (assuming no changes in reorganization energies). Another reason for the change of the intramolecular electron-transfer rate with pH could be a reduction in electronic coupling between the heme and ruthenium centers, involving either the His-18-to-Pro-30 hydrogen bond along the putative electron-transfer pathway or a conformational change induced by the $N_R \rightarrow N_R^*$ transition or even another transition not directly related to $N_R \rightarrow N_R^*$.

Comparison of the pH effect on Ru-to-Fe electron transfer with that in the opposite direction help may differentiate between the different alternatives. Bechtold et al.²⁴ measured the rate of intramolecular electron transfer in (NH₃)₅Ru-Cyt *c* as a function of pH. Their data above pH 6, rescaled for clarity, are also shown in Figure 3. At pH 9.55 the observed intramolecular rate drops to 36 s⁻¹, from an average of 56 ± 5 s⁻¹ between pH 5.13 and 8.56. In addition, at pH 9.55 the signal amplitude corresponding to Ru-to-Fe electron transfer was only 10% of that obtained at lower pH. At pH 11, direct reduction of the heme was observed, but no intramolecular reduction of the heme was seen. These observations are consistent with an increasing equilibrium fraction of the alkaline ferricytochrome

TABLE 3: Reduction Potentials ($E_{1/2}$, V vs NHE) for Three Ruthenium Ammine Complexes in Phosphate Buffer and Other Media by Cyclic Voltammetry

complex	phosphate ^a	Tris ^b	tosylate ^c	other
$[(\text{NH}_3)_6\text{Ru}]^{3+/2+}$	0.022	0.048	0.050	0.051 ^d
$[(\text{NH}_3)_5\text{Ru}(3,5\text{-lutidine})]^{3+/2+}$	0.234	0.264 ^e	0.255	0.260 ^f
$[(\text{NH}_3)_5\text{Ru}(\text{isonicotinamide})]^{3+/2+}$	0.348	0.379	0.375	

^a Buffer: 50 mM phosphate, 0.10 M sodium formate, pH 7.0.^b Buffer: 50 mM TrisHCl, 0.10 M sodium formate, pH 7.0. ^c 0.10 M *p*-toluenesulfonic acid, 0.10 M potassium *p*-toluenesulfonate. Data from ref 27. ^d 0.10 M NaBF₄. Reference 28. ^e Buffer: 50 mM TrisHCl, 0.10 M KCl, pH 7.0. ^f 0.10 M KCl.

c, which has a reduction potential²³ of -0.205 V vs NHE at pH 10.0, well below that of the pendant $(\text{NH}_3)_5\text{Ru}$ moiety. Although the rate reduction at pH 9.55 would tend to support the above hypothesis concerning reduced coupling at higher pH over the ligand deprotonation hypothesis (which would speed up this reaction by lowering the potential of the ruthenium center), there is insufficient evidence to reach a conclusion at this time. In addition, the pK_a for ligand deprotonation is likely to be higher in the pentaammine case. Further investigation of the pH effect in the $L = \text{NH}_3$ case, using the oxidative pulse radiolysis scheme described above, may resolve some of the above ambiguities.

Effect of Phosphate on ET Thermodynamics, Rates and Activation Parameters. Armstrong et al.²⁵ observed a negative shift of ~ 10 – 28 mV in the reduction potential of the $[(\text{NH}_3)_5\text{Ru}(\text{his})]$ center in three Ru-modified proteins when measured in 0.10 M phosphate buffer as compared to measurements in a mixed buffer system lacking phosphate. We have also observed differences in rate constants obtained in phosphate versus other buffers. For example, in the course of our investigations of $\text{Co}(\text{ox})_3^{3-}$ oxidation of ruthenium-modified cytochromes,²⁶ the observed rates for endoergic Fe-to-Ru electron transfer in Hh $(\text{NH}_3)_5\text{Ru}$ –Cyt *c* was found to be 0.53 s^{-1} in 50 mM cacodylate buffer, whereas the rate in 50 mM pH 7 phosphate buffer² is 0.40 s^{-1} , implying that the reduction potential of the ruthenium site is lower in the phosphate case.

Table 3 summarizes the results of cyclic voltammetry measurements on three model ruthenium ammine compounds in phosphate buffer and other media at room temperature. In the presence of 50 mM phosphate buffer the reduction potentials of the ruthenium complexes are shifted lower by 20–30 mV. The same shift was observed when the Tris buffer solutions in the second column were spiked with 50 mM phosphate. Similar but smaller reductions in the driving force for Fe-to-Ru intramolecular electron transfer in the presence of phosphate are evident in the comparison between differences in DPV peak potentials in phosphate and Tris media listed in Table 4. Also listed in Table 4 are the observed intramolecular electron-transfer rates and activation parameters in the Tris medium. The $L = 4$ -ethylpyridine, 3,5-lutidine, and pyridine rates are about 30%

faster in Tris buffer than in phosphate, while the isonicotinamide rate is 10% faster. Small, partially compensatory changes in the activation parameters are observed. In addition, a trend appears along the sequence $L = \text{etpy}$, lut, py, isn where the difference between ΔH^\ddagger for phosphate and that for Tris increases while the difference in $-\Delta S^\ddagger$ changes in the opposite direction. Overall, though the effect of phosphate is small, it must be considered in the making of detailed comparisons.

Summary. Intramolecular electron transfer in ammineruthenium-modified horse heart cytochrome *c* is reversible, and the driving force dependencies of the electron transfer rates and activation parameters follow the predictions of Marcus–Hush theory. Electron transfer from the heme center to the pendant ruthenium group is endothermic and driven by a large increase in entropy, most likely due to the release of electrostricted water around the ruthenium complex. Only in the case of $L = \text{NH}_3$ (and presumably, $\text{H}_2\text{O}/\text{OH}^-$) is the endothermicity large enough to override the entropy increase at room temperature and reverse the direction of spontaneous electron transfer.

We have examined the effect of phosphate ion binding on the reduction potentials of pendant ruthenium ammine groups which were reported by other workers. Under the conditions frequently used to study electron transfer in ruthenium-derivatized proteins the phosphate-induced change in driving force can be as large as 30 meV, which may change the observed rates by as much as 30%. These results underscore the importance of careful consideration of medium-specific effects when making detailed rate comparisons.

Investigation of the pH dependence of intramolecular electron transfer in $(\text{NH}_3)_4\text{Ru}(\text{isn})\text{Cyt } c$ revealed a dramatic decrease in rate with a midpoint at pH 9.1, which happens to correspond with the pK for the transition between the normal and alkaline forms of horse heart ferricytochrome *c*. Previous work²⁴ showed a large increase in the intramolecular electron-transfer rate in $(\text{NH}_3)_5\text{RuCyt } c$ below pH 3.2. Detailed work on pH dependencies could shed more light on the roles of hydrogen bonding and conformation on the electron-transfer process. Such information would be of value for the refinement of electron-transfer pathway models. Electron-transfer measurements can, in turn, provide information about protein stability and conformational interconversion rates.

Acknowledgment. This research was performed in part at Brookhaven National Laboratory under Contract DE-AC02-76CH00016 with the U.S. Department of Energy and supported by its Division of Chemical Sciences, Office of Basic Energy Sciences. The research at Rutgers University was supported by the Center for Advanced Food Technology (CAFT) at Rutgers University, the National Science Foundation (Grant CHE 840552) and the Charles and Johanna Busch Foundation.

Supporting Information Available: Graph of absorbance vs time traces for oxidative pulse radiolysis of $(\text{NH}_3)_5\text{RuCyt } c$,

TABLE 4: DPV Peak Potential Differences in Phosphate and Tris Buffers and Observed Intramolecular Electron-Transfer Rates and Activation Parameters in Tris Buffer for Several Ruthenium-Modified Cytochromes

complex	$\Delta E_{\text{peak}}(\text{Ru} - \text{Cyt } c) \text{ (mV)}$		$k_{\text{obs}}^b \text{ (s}^{-1}, 25^\circ\text{C)}$	$\Delta H^\ddagger^b \text{ (kcal/mol)}$	$\Delta S^\ddagger^b \text{ (eu)}$
	Phosphate ^a	Tris ^{b,c}			
$(\text{NH}_3)_5\text{Ru} - \text{Cyt } c$	-124 ± 1	-97			
$(\text{NH}_3)_4(\text{etpy})\text{Ru} - \text{Cyt } c$			105 ± 4	9.2 ± 0.1	-18.5 ± 0.3
$(\text{NH}_3)_4(\text{lut})\text{Ru} - \text{Cyt } c$	$+85 \pm 1$	$+88 \pm 1$	110 ± 3	9.3 ± 0.1	-18.0 ± 0.2
$(\text{NH}_3)_4(\text{py})\text{Ru} - \text{Cyt } c$	$+113 \pm 1$	$+122 \pm 1$	160 ± 8	8.6 ± 0.1	-19.7 ± 0.3
$(\text{NH}_3)_4(\text{isn})\text{Ru} - \text{Cyt } c$	$+182 \pm 1$	$+190 \pm 1$	480 ± 40	6.8 ± 0.1	-23.6 ± 0.4

^a Buffer: 50 mM potassium phosphate, pH 7.0, 25 °C. Data from the Supporting Information. Average of four or more observations. ^b Buffer: 10 mM TrisHCl, 10 mM NaN₃, 80 mM NaClO₄, pH 7.0. ^c Pressure: 50 atm, however extrapolation of the best fit lines to 1 atm result in corrections of less than +1 mV. Data from ref 6. Average of four observations except $L = \text{NH}_3$ where there was only one. Temperature: 25 °C.

graphs and data summarizing nonisothermal differential pulse voltammetry determination of the redox thermodynamics of *trans*-(NH₃)₄Ru(L)Cyt c, L = NH₃, 3,5-lutidine, pyridine and isonicotinamide, and Eyring plots for intramolecular electron transfer in phosphate and Tris buffers for L = 4-ethylpyridine, 3,5-lutidine, pyridine and isonicotinamide (11 pages). Ordering information is given on any current masthead page.

References and Notes

- (1) Sun, J.; Wishart, J. F.; Gardineer, M. B.; Cho, M. P.; Isied, S. S. *Inorg. Chem.* **1995**, *34*, 3301–3309.
- (2) Sun, J.; Wishart, J. F.; Isied, S. S. *Inorg. Chem.* **1995**, *34*, 3998–4000.
- (3) Moriera, I.; Sun, J.; Cho, M. O.-K.; Wishart, J. F.; Isied, S. S. *J. Am. Chem. Soc.* **1994**, *116*, 8396–8397.
- (4) Winkler, J. R.; Gray, H. B. *Chem. Rev. (Washington, D.C.)* **1992**, *92*, 369–379.
- (5) Mines, G. A.; Bjerrum, M. J.; Hill, M. G.; Casimiro, D. R.; Chang, I.-J.; Winkler, J. R.; Gray, H. B. *J. Am. Chem. Soc.* **1996**, *118*, 1961–1965.
- (6) Sun, J.; Wishart, J. F.; van Eldik, R.; Shalders, R. D.; Swaddle, T. W. *J. Am. Chem. Soc.* **1995**, *117*, 2600–2605.
- (7) Wishart, J. F.; van Eldik, R.; Sun, J.; Su, C.; Isied, S. S. *Inorg. Chem.* **1992**, *31*, 3986–3989.
- (8) Fenwick, C.; Marmor, S.; Govindaraju, K.; English, A. M.; Wishart, J. F.; Sun, J. *J. Am. Chem. Soc.* **1994**, *116*, 3169–3170.
- (9) Sun, J.; Su, C.; Wishart, J. F. *Inorg. Chem.*, **1996**, *35*, 5893–5901.
- (10) Bailar, J. C. Jr.; Jones, E. M. *Inorg. Synth.* **1939**, *1*, 37.
- (11) Yocom, K. M.; Shelton, J. B.; Shelton, J. R.; Schroeder, W. A.; Worosila, G.; Isied, S. S.; Bordignon, E.; Gray, H. B. *Proc. Natl. Acad. Sci. U.S.A.* **1982**, *79*, 7052–7055.
- (12) Margoliash, E.; Frohwirt, N. *Biochem. J.* **1959**, *71*, 570–572.
- (13) Isied, S. S.; Kuehn, C.; Worosila, G. *J. Am. Chem. Soc.* **1984**, *106*, 1722–1726.
- (14) Ram, M. S.; Stanbury, D. M. *J. Phys. Chem.* **1986**, *90*, 3691–3696.
- (15) Stanbury, D. M. *Adv. Inorg. Chem.* **1989**, *33*, 69–138.
- (16) If L = NH₃, the energetically favorable direction of reaction 7 is reversed.
- (17) Marcus, R. A.; Sutin, N. *Biochim. Biophys. Acta* **1985**, *811*, 265–322.
- (18) Recently, an EPR and NMR study^{18a} of the influence of *trans* ligands on d_π–π(imidazole) orbital mixing in *trans*-(NH₃)₄Ru^{III}(L)(im)] complexes was published. The report indicated that the coupling between the ruthenium d_π orbitals and the imidazole C5 carbon attached to the rest of the protein is modulated by the π-donor or π-acceptor properties of the *trans* ligand. However, this phenomenon would diminish the coupling by only 20% over the range of L = NH₃ to isonicotinamide, an effect which is too small to discern in our data. Furthermore, the opposing effect of reduced reorganization energy for L = (etpy, lut, py, and isn) has a much larger influence on the observed rates. In ref 18a the authors also calculate a larger upper limit (which would be a factor of 5.2 favoring NH₃ over isn) based on the assumption that the d_π orbital is not the highest t_{2g} orbital in the pyridine and isonicotinamide cases. However, recent work by Shin et al.^{18b} indicates that d_π would always be highest in this series of complexes. (a) LaChance-Galang, K. J.; Doan, P. E.; Clarke, M. J.; Rao, U.; Yamano, A.; Hoffman, B. M. *J. Am. Chem. Soc.* **1995**, *117*, 3529–3538. (b) Shin, Y.-g. K.; Brunschwig, B. S.; Creutz, C.; Newton, M. D.; Sutin, N. *J. Phys. Chem.* **1996**, *100*, 1104–1110.
- (19) In the case of [Ru(NH₃)₄(L)]²⁺ (L = NH₃), λ_{Ru} was empirically estimated to be 0.2 eV higher than in the cases where L is a substituted pyridine, due to an increase in the outer-sphere contribution as a result of the smaller radius.^{19a} The effect of this correction is to lower the calculated rate constant for L = NH₃ by a factor of 2.6. (a) Sutin, N. In *Tunneling in Biological Systems*; Chance, B., DeVault, D. C., Frauenfelder, H., Marcus, R. A., Schrieffer, J. B., Sutin, N., Eds.; Academic Press: New York, 1979; pp 201–227.
- (20) Therien, M. J.; Selman, M. A.; Gray, H. B.; Chang, I.-J.; Winkler, J. R. *J. Am. Chem. Soc.* **1990**, *112*, 2420–2422.
- (21) An empirical fit to the line defined by the other complexes obtains estimates of λ₁₂ = 1.3 eV and λ_{Ru} = 1.6 eV for L = *N*-methylpyrazinium. The increase in λ_{Ru} would be attributable to the outer-sphere contribution.
- (22) Theorell, H.; Åkesson, A. *J. Am. Chem. Soc.* **1941**, *63*, 1812–1818.
- (23) Barker, P. D.; Mauk, A. G. *J. Am. Chem. Soc.* **1992**, *114*, 3619–3624.
- (24) Bechtold, R.; Gardineer, M. B.; Kazmi, A.; van Hemelryck, B.; Isied, S. S. *J. Phys. Chem.* **1986**, *90*, 3800–3804.
- (25) Armstrong, F. A.; Butt, J. N.; Govindaraju, K.; McGinnis, J.; Powls, R.; Sykes, A. G. *Inorg. Chem.* **1990**, *29*, 4858–4862.
- (26) Sun, J. Ph.D. Dissertation, Rutgers, the State University of New Jersey, 1993.
- (27) Matsubara, T.; Ford, P. C. *Inorg. Chem.* **1976**, *15*, 1107–1110.
- (28) Lim, H. S.; Barclay, D. J.; Anson, F. C. *Inorg. Chem.* **1972**, *11*, 1460–1466.